COMPUTATIONAL
ANDSTRUCTURAL
BIOTECHNOLOGY
JOURNAL

Conformational ensemble of the TNF-derived peptide solnatide in solution

Pau Martin-Malpartida [a], Silvia Arrastia-Casado [b], Josep Farrera-Sinfreu [b], Rudolf Lucas [c], Hendrik Fischer [d], Bernhard Fischer [d], Douglas C. Eaton [e], Susan Tzotzos [d,*], Maria J. Macias [a,f,*]

[a] Institute for Research in Biomedicine, The Barcelona Institute of Science and Technology, Baldiri Reixac, 10, Barcelona 08028, Spain
[b] BCN Peptides S.A. Pol. Ind. Els Vinyets-Els Fogars, Barcelona, Spain
[c] Vascular Biology Center, Dept of Pharmacology and Toxicology, Medical College of Georgia at Augusta University, Augusta, GA, USA
[d] APEPTICO Forschung und Entwicklung GmbH, Mariahilferstraße 136, 1150 Vienna, Austria
[e] Department of Medicine, Emory University School of Medicine, Atlanta, GA, USA
[f] Institució Catalana de Recerca i Estudis Avançats (ICREA), Passeig Lluís Companys 23, Barcelona 08010, Spain

ARTICLE INFO

ABSTRACT

Tumor necrosis factor (TNF) is a homotrimer that has two spatially distinct binding regions, three lectin-like domains (LLD) at the TIP of the protein and three basolaterally located receptor-binding sites, the latter of which are responsible for the inflammatory and cell death-inducing properties of the cytokine. Solnatide (a.k.a. TIP peptide, AP301) is a 17-mer cyclic peptide that mimics the LLD of human TNF which activates the amiloride-sensitive epithelial sodium channel (ENaC) and, as such, recapitulates the capacity of TNF to enhance alveolar fluid clearance, as demonstrated in numerous preclinical studies. TNF and solnatide interact with glycoproteins and these interactions are necessary for their trypanolytic and ENaC-activating activities. In view of the crucial role of ENaC in lung liquid clearance, solnatide is currently being evaluated as a novel therapeutic agent to treat pulmonary edema in patients with moderate-to-severe acute respiratory distress syndrome (ARDS), as well as severe COVID-19 patients with ARDS. To facilitate the description of the functional properties of solnatide in detail, as well as to further target-docking studies, we have analyzed its folding properties by NMR. In solution, solnatide populates a set of conformations characterized by a small hydrophobic core and two electrostatically charged poles. Using the structural information determined here and also that available for the ENaC protein, we propose a model to describe solnatide interaction with the C-terminal domain of the ENaCα subunit. This model may serve to guide future experiments to validate specific interactions with ENaCα and the design of new solnatide analogs with unexplored functionalities.

© 2022 The Author(s). Published by Elsevier B.V. on behalf of Research Network of Computational and Structural Biotechnology. This is an open access article under the CC BY-NC-ND license (http://creativecommons.org/licenses/by-nc-nd/4.0/).

1. Introduction

Human tumor necrosis factor (TNF) forms a 51 kD homotrimer, with three lectin-like domains (LLD) located at the apex of the molecular structure, one at the tip of each subunit, spatially separated from the basolaterally located receptor-binding sites (Fig. 1A, B) [1–4]. TNF has been described as a "moonlighting" protein because it has several physiological functions within the same polypeptide chain but through different binding sites [5,6]. It was initially discovered as an anticancer agent, and later, the role of TNF and its family members in diverse pathologies, including neurologic, metabolic, cardiovascular, pulmonary, and autoimmune diseases, was characterized [7]. TNF is a pleiotropic cytokine with cell death-inducing and inflammatory effects on mammalian cells
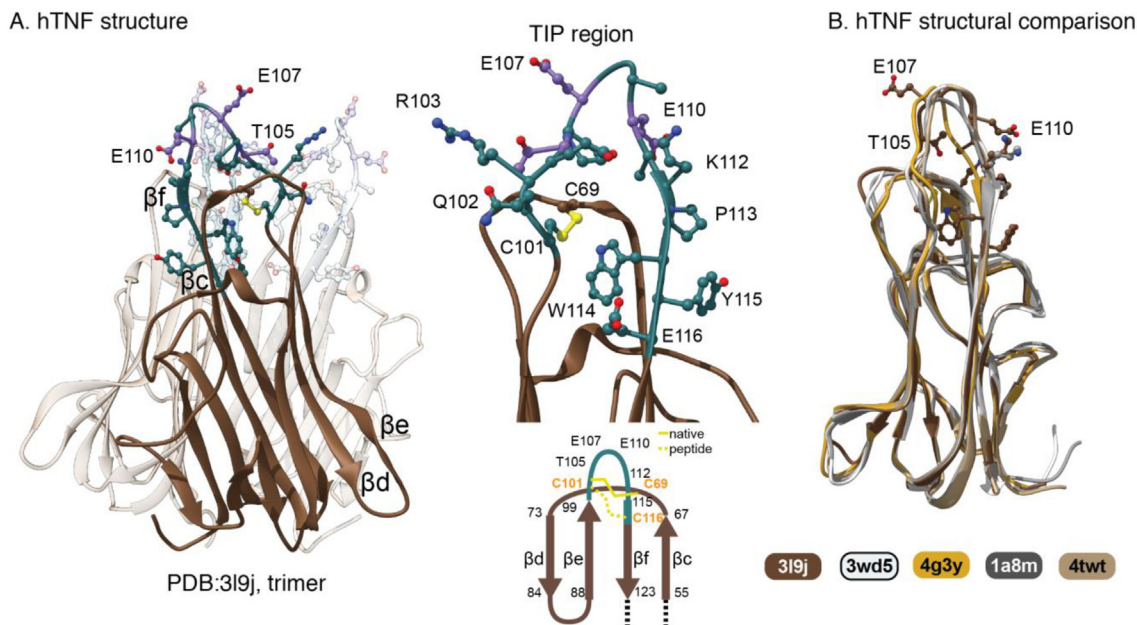
Fig. 1. hTNF trimer and the three lectin-like domains. A. The region corresponding to the scaffold used to design the solnatide peptide is highlighted in teal. A schematic representation of the secondary structure is shown below. B. Superposition of several TNF structures displaying the conformational variability of the loop.

mediated through binding to two types of receptors [5,8]. TNF plays a major role in innate defence against bacterial, fungal, parasitic and viral infections [6]. Less well-known is its lectin-like activity, which is completely dissociable from its death-inducing and inflammatory role. The lectin-like activity of TNF causes activation of the amiloride-sensitive epithelial sodium channel (ENaC) in the alveolar epithelium and also in lung microvascular endothelial cells [9–11].

Spatial separation of the functions of TNF into distinct regions in the molecule might explain the apparent contradictory roles of this cytokine, which, on the one hand, exacerbates inflammation and edema formation through its receptor-binding domains and, on the other hand, activates edema reabsorption through its lectin-like domain [1,5]. Residues Cys101-Glu116 of wild-type human TNF (hTIP) participate in the activation of ENaC [3,12]. The lectin-like activity of TNF (TIP) domain of TNF was mapped 28 years ago in view of its trypanolytic effect on purified bloodstream forms of *Trypanosoma brucei brucei* [3]. Subsequently, its role in the activation of amiloride-sensitive sodium transport in mammalian lung cells [9,10] and its edema-reducing capacity were also identified [10,13].

The synthetic 17-mer cyclic peptide solnatide, also known as human TIP peptide or AP301, mimics the LLD of human TNF without having the receptor-binding site responsible for the inflammatory properties of this cytokine [1,3,13]. Solnatide and its mouse analog mTIP peptide have been shown to improve alveolar fluid clearance and reduce extravascular lung water in several rodent models of flooded lungs [1,13], in a rabbit model of endotoxin/exotoxin-induced lung injury [14], and in a mouse model of pneumonia [11]. Solnatide is currently being evaluated in a Phase II clinical trial (EU Clinical Trials Register, EudraCT No. 2017-003855-47; ClinicalTrials.gov Identifier: NCT03567577) as a novel agent to study the safety and preliminary efficacy in patients with moderate-to-severe acute respiratory distress syndrome (ARDS). Moreover, a completed pilot study of treatment of severe COVID-19 patients with ARDS with solnatide is currently being evaluated (EU Clinical Trials Register, EudraCT No. 2020-001244-26). In a previous "proof-of-concept" study in patients suffering from acute

lung injury, the analysis of a subgroup of patients with the highest sequential organ failure assessment (SOFA) scores revealed reduced extravascular lung water following treatment with inhaled solnatide [15]. A recent pilot study in patients with primary graft dysfunction following lung transplantation who received inhaled solnatide showed improved gas exchange and reduced need for mechanical ventilation, thereby bringing about a shorter stay in the intensive care unit [16].

TNF -through its LLD- and solnatide -a LLD mimic- activate ENaC, which is expressed at the apical plasma membrane of epithelial and endothelial cells in various tissues and organs, including lungs, colon, kidneys [17,18]. This activity has been measured electrophysiologically as an increase in amiloride-sensitive sodium current in cells expressing ENaC [11,12,19,20]. ENaC is the rate-limiting step for Na^+ uptake and it plays a critical role in lung fluid clearance in physiological and disease conditions [17,21]. The function of ENaC is determined by the number of channels expressed at the surface membrane (N), which is regulated by membrane insertion, ubiquitination and degradation or retrieval, as well as on the activity of individual channels, defined by their open probability Po [22]. TNF/solnatide-dependent ENaC-activation promotes the channel's open state, thus affecting the regulation of Na^+ and water homeostasis [10,11,19,23,24]. Na^+ ions passively enter alveolar epithelial cells through apically located ENaC and are actively removed by the basolaterally located Na^+-K^+-ATPase. This unidirectional Na^+ transport creates an osmotic gradient that causes water to flow in the same direction [25]. By increasing the Po of ENaC, solnatide increases Na^+ uptake across the alveolar epithelium. Water follows the ensuing osmotic gradient out of the alveolar lumen into the interstitial space, eventually reaching the blood and lymphatic systems.

ENaC is structured as a heterotrimeric molecule composed of three subunits (α, β and γ), each containing a large extracellular domain, two transmembrane (TM) regions, and two flexible intracellular N- and C-terminal regions [26,27]. The precise molecular mechanism by which solnatide interacts with ENaC and increases its Po is currently unknown, although a combined *in vitro-in vivo* study has shown that solnatide binds to the intracellular C-

terminal domain of the α–subunit of ENaC (ENaCα) [11]. This binding favors continued expression of ENaCα and the complex formation between the channel, the myristoylated alanine-rich C kinase substrate (MARCKS) and phosphatidylinositol bisphosphate (PIP2), both necessary for maintaining the open conformation of ENaC [11,23]. Two residues (Val567 and Glu568) at the end of the second transmembrane region (TM2) of human ENaCα have been postulated to play an important role in solnatide binding because their mutation to alanine significantly reduces the stimulatory effect of the peptide on complex formation between ENaC and MARCKS [23]. Moreover, the capacity of both solnatide and TNF to enhance amiloride-sensitive sodium current is lost when three essential residues, namely Thr6/105, Glu8/107 and Glu11/110 (numbers refer to solnatide and human TNF respectively), are each replaced by alanine [10,12]. These three residues are also critical for the edema-reabsorbing properties and trypanolytic effects of the lectin-like domain [3,10,13].

TNF and solnatide interact specifically with N,N'-diacetyl chitobiose and high mannose-containing carbohydrate groups of glycoproteins, and this interaction is necessary for their trypanolytic and ENaC-activating effects [3,9,28]. Interestingly, a linear form of the hTIP peptide still binds to N,N'-diacetylchitobiose, indicating that cyclization is not necessary for the peptide-carbohydrate interaction [29]. The mutated variant of solnatide containing the three essential residues 6, 8 and 11 replaced with alanine retains the capacity to bind to N,N'-diacetylchitobiose but shows greatly reduced affinity compared to solnatide [29].

These binding results with ENaCα and N,N'-diacetlychitobiose suggest that solnatide (hTIP peptide, AP301) has different binding sites to exert its polyvalent function in cells. However, the lack of structural information regarding the conformational ensemble populated by the peptide in solution has prevented the research community from proposing structure-based hypotheses to describe its binding properties. To bridge this knowledge gap and to open up the possibility of docking studies with targets and designing new analogs with unexplored functionalities, we set out to study solnatide folding properties in solution by NMR. The conformational ensembles determined allowed us to identify three regions as potential binding platforms to interact with different targets. We compared these sites to the LLD in hTNF described in available crystal structures, thereby revealing conserved and distinct features that are essential for the bioactivity of the peptide. Based on the conformational properties of solnatide, we also propose how it might interact with sugars and with ENaCα through hydrophobic and electrostatic interactions. These hypotheses will pave the way for designing new experimental approaches to unveiling the activation mechanism of ENaC by solnatide, elucidation of solnatide's lectin-like properties, as well as its role in enhancing edema reabsorption in patients.

2. Material and methods

2.1. Peptide synthesis

Solnatide (a.k.a. TIP peptide, AP301) was prepared using a linear stepwise solid-phase peptide synthesis and following the Fmoc/tBu strategy, essentially as previously described [30–32]. Chain elongation was achieved by repetitive cycles of Fmoc removal and amino acid coupling. The completeness of each coupling was checked by the Kaiser (Ninhydrin) and/or Chloranyl tests. The crude peptide was obtained after acidolytic treatment and subsequent oxidation. Finally, the crude product was purified by preparative reverse-phase HPLC and counter-ion exchanged to obtain the final product in the acetate form. Finally, the product was isolated by lyophilization and stored at −20 °C. The cyclic 17-residue peptide showed a purity of 99.5%, as determined by a validated HPLC protocol.

2.2. NMR methods

NMR experiments were recorded on a Bruker Avance III 600-MHz spectrometer (IRB Barcelona) equipped with a quadruple (^{1}H, ^{13}C, ^{15}N, ^{31}P) resonance cryogenic probe head and a z-pulse field gradient unit at 290 K using a 1 mM solution of peptide. 1D proton spectra were recorded with a sweep width of 12,000 Hz and 32 k data points. A total of 16 scans were accumulated with an acquisition time of 2.05 s. A Watergate w5 composite pulse was used to suppress the water signal. Presaturation was used in samples dissolved in D_2O. 2D-TOCSY and NOESY experiments were carried out in 90% H_2O/10% D_2O and in 100% D_2O and used to assign the spin systems corresponding to the peptide resonances, as previously described [33,34]. For the 2D-NOESY experiments, mixing times of 200 and 100 ms were used to minimize the impact of spin-diffusion in the NOE assignments. Spin-locking fields of 8 kHz and 50 ms mixing time were used for the 2D-TOCSY experiments. All 2D spectral widths were 8000 Hz. The data size was 512 points in F1, indirect dimension, and 2048 points in F2, direct dimension. For each F1 value, 48 and 32 transients were accumulated in the NOESY and TOCSY experiments, respectively. Data were processed with a combination of exponential and shifted sine-bell window functions for each dimension, followed by automated baseline and phase correction using TopSpin 3.5 (© Bruker 2020). The 512 × 2 k data matrices were zero-filled to 2 k × 2 k (NOESY and TOCSY).

2.3. Structure calculation

We identified the characteristic spin system of each residue in the sequence using the 2D TOCSY experiment. Each spin system was connected to the following one via NOEs observed from the side-chain of a given residue (i) to the amide proton of the following residue (i + 1), as well as from the amide proton of (i) to the amide of (i + 1), as previously described [35,36]. Full spin analysis and NOE assignment were carried out manually using CARA software [37]. Distance restraints derived from the NOESY experiments were used for the NMR-based model building of the peptide in solution using unambiguously assigned peaks exclusively and the program CNS 1.2 (Crystallography and NMR system) [38,39]. The protocol consisted of implicit water-simulated annealing of 200 structures using 8,000 cooling steps, followed by an explicit water refinement during 1200 steps, essentially as described [32,40]. The top 40 models were further refined using the Rosetta package, with the FastRelax protocol with all NMR constraints and the cst_fa_weight parameter set to 2 [41]. All structures were represented using Chimera version 1.13 [42].

2.4. Docking

RosettaDock r280[43] was used to dock the minimum-energy NMR conformer of solnatide to the ENaCα helix predicted by AlphaFold_v2 (residues 563–595). Both structures were prepacked using the Rosetta docking_prepack_protocol r280 with the default settings to perform side chain optimization of each component of the complex. No preferred starting orientation was selected. As the docking protocol was run without using a lipidic membrane, all simulations in which the solnatide molecule was bound at the hydrophobic side of the helix were discarded and the complex with the lowest energy bound to the polar face of the helix was selected (Fig. 5b). The docking protocol was as follows: -dock_pert 3 8 -ex1 -ex2aro -score:docking_interface_score 1 -nstruct 10,000 -randomize2 -uniform_trans 200 -spin. The energy values for that structure were:

P. Martin-Malpartida, S. Arrastia-Casado, J. Farrera-Sinfreu et al.

Computational and Structural Biotechnology Journal 20 (2022) 2082–2090

Total_score: −45.542; I_sc: −9.546. According to the RosettaDock documentation, the optimal values for I_sc are in the range of −5 to −10.

3. Results

3.1. Peptide synthesis and previous knowledge of the lectin-like (TIP) domain

Solnatide is a cyclic peptide that mimics the lectin-like (TIP) domain of human TNF cytokine. The TNF protein folds as a homotrimeric molecule, where the monomers adopt an edge-to-face packing (Fig. 1A) [44]. The 17-residue solnatide sequence is based on the native Pro100-Glu116 fragment of hTNF (UniProt code, P01375). In the TNF structure, this region belongs to a fragment between β strands e and f (Fig. 1B). In solnatide, the hTIP sequence [3] was altered by replacing Pro100 and Glu116 with Cys, and Cys101 with Gly. The Cys residues introduced were used to generate a head-to-tail cyclic peptide via a disulfide bond.

### 3.2. Chemical shift assignment of the solnatide peptide

For structural studies by solution NMR, we prepared the 17-residue solnatide sequence using standard Fmoc/tBu solid-phase peptide synthesis (as described in the Methods section). To explore the conformational ensemble of solnatide in solution, we performed 2D ^1H–^1H TOCSY and NOESY and ^1H–^{13}C HSQC experiments to obtain the full ^1H and ^{13}C assignment. To determine the folding properties, we acquired several NOESY experiments covering a range of mixing times in H_2O and D_2O. The well-dispersed signals in the 2D TOCSY/NOESY experiments allowed us to identify all residues, which were sequentially connected by the presence of unambiguous sequential and medium-range NOEs following standard protocols [36]. The presence of the internal disulfide bond was confirmed by the characteristic Cβ chemical shifts of the two Cys residues observed in the 2D HSQC experiment [45]. The monomeric properties of the peptide were corroborated by its molecular weight determined by Mass Spectrometry and by the pattern of NOEs, consistent with a cyclic peptide structure, with the N- and C-termini in close proximity (Fig. 2A-D).

The analysis of the NMR datasets allowed us to collect a set of sequential and medium range restraints to calculate an ensemble of conformations sampled by the peptide in solution. Only six residues (Arg4, Thr6, Lys13, Pro 14, Trp15 and Tyr16) participate in side-chain to side-chain interactions. For instance, we detected a set of NOEs between the aromatic ring of Trp15 and Tyr16 with Lys13 and Pro14 side-chains and also between Trp15 and Tyr16 aromatic rings and between Tyr16 and Arg4. Thr6 also showed weak NOEs to Trp15. The contacts between the two aromatic rings are probably enhanced by the cyclic nature of the peptide, which somehow introduces a turn after residue 16 to form the Cys1-Cys17 disulfide bond. We observed that the two proline residues (at position 7 and 14) populate cis/trans configurations, with trans being the most abundant (Fig. 2B).
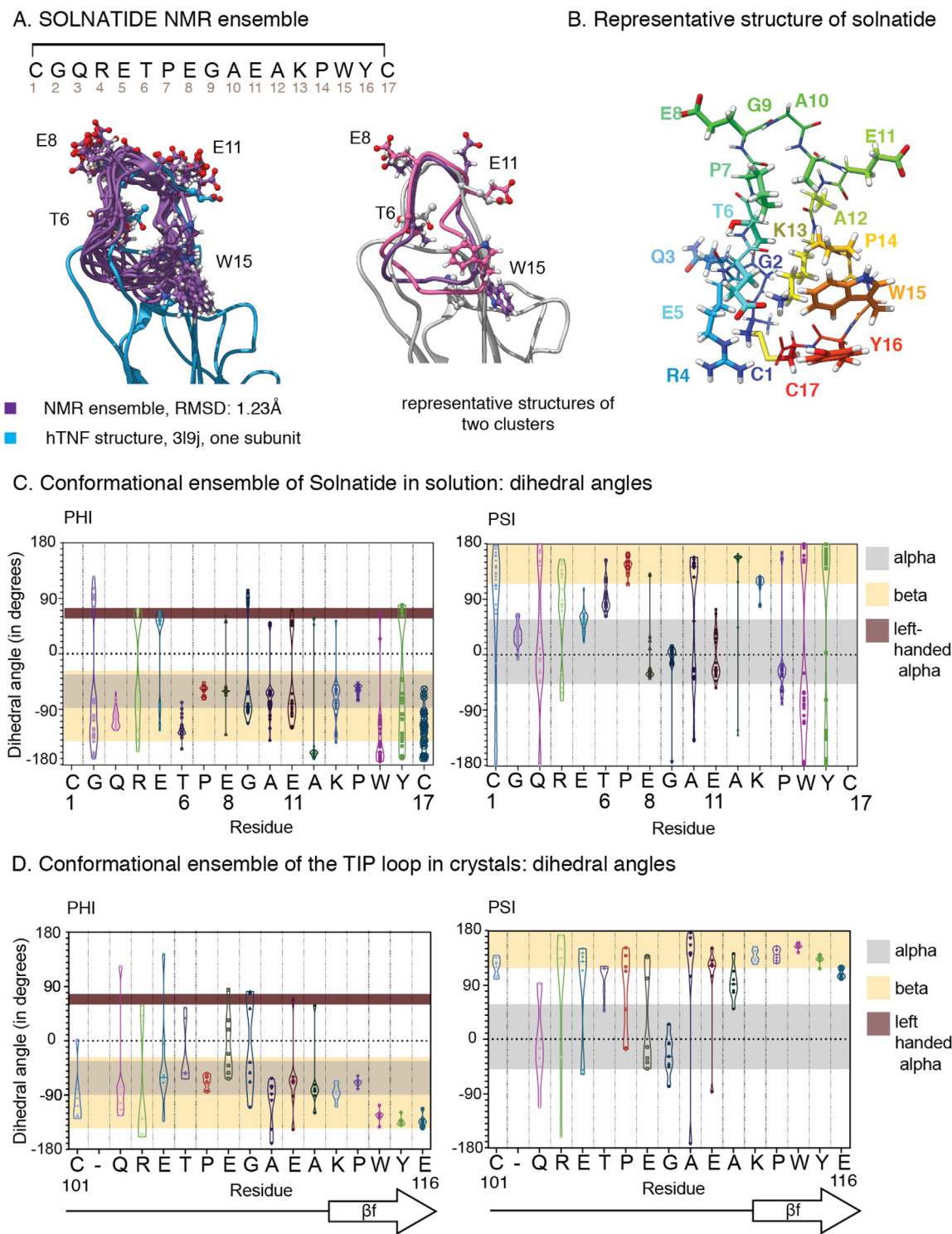
3.3. Conformational ensemble of solnatide in solution using NMR restraints. Comparison to TNF structures

The conformational ensemble of the peptide was determined through the combination of the Crystallography & NMR system software suite (CNS) and Rosetta, using all experimentally derived NMR restraints during both processes. We observed that the additional refinement step with Rosetta yields more accurate NMR ensembles than those using standard refinement protocols only, as previously described for other protein systems [41,46].

We first generated 400 structural models using the experimental data and CNS with a refinement step in the presence of explicit solvent [38,39,47]. After this calculation, we ranked the generated models based on energy values and on the absence of restraint violations. The top 40 models were further refined using the Rosetta package, guiding this refinement process with the requirement to fulfil the assigned experimental constraints. The unrefined and refined structural ensembles are very similar but the latter display a clear improvement of backbone dihedral angles and side-chain rotamers (as determined by PROCHECK [48]). In solution, the conformational ensemble adopted by solnatide reveals a global fold that resembles that of the hairpin in the native TNF context, as shown by the overlays of the top 20 conformers representing selected or all the side-chains, (Fig. 3A, B). The family of conformations have two distinct sections according to the flexibility: resi-
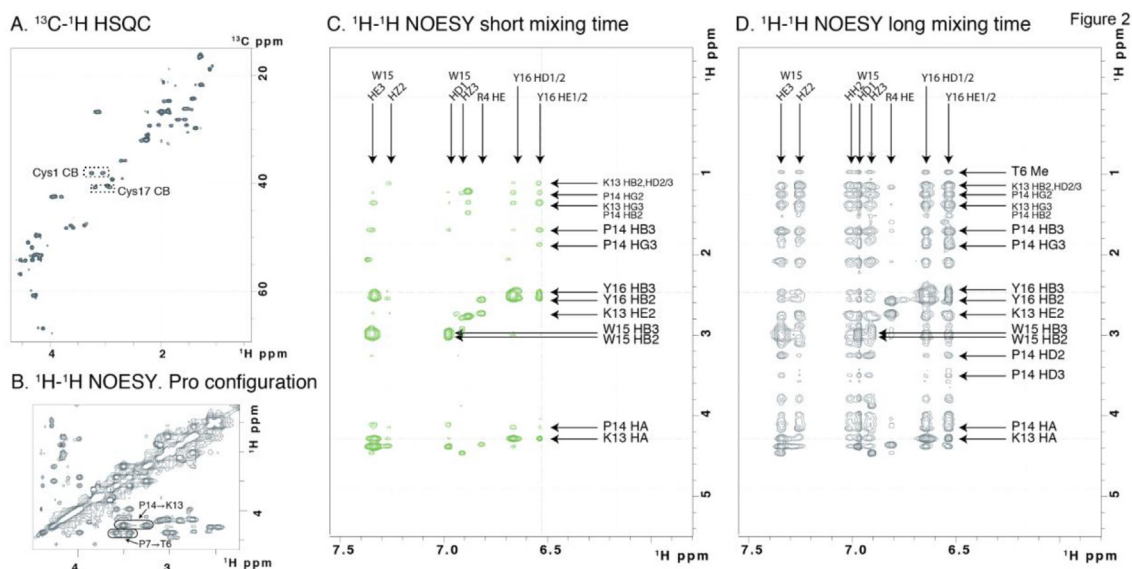
Fig. 2. Characteristic chemical shifts and NOEs observed for solnatide. A. HSQC displaying the aliphatic region of the peptide. The characteristic resonances of the oxidized Cys are highlighted. The chemical shifts corresponding to all residues are included in Supplementary Tables 1 and 2. B. Characteristic NOE pattern of the Proline trans configuration. C and D. NOEs observed between the aromatic rings of Trp15 and Tyr16 with Thr6 (weak) and with Lys13 and Pro14.

Fig. 3. NMR ensemble of solnatide. A. NMR ensemble of the peptide (violet) superimposed to the corresponding region of the native TNF protein (blue). Two selected conformations are shown superimposed to the TNF TIP region. Conserved side-chains are indicated (numbers refer to solnatide). B. The lowest energy conformation with all side-chains shown. The peptide is colored N->C Rainbow starting with blue, till red. C. Conformational variability of the 20 best structures of solnatide determined here (PDB ID: 7qlf). D. Similar analysis of seven TNF structures (PDB ID: 3l9j, 3wd5, 4g3y, 1a8m, 4twt, 1tnf, 5m2i, 5m2m). The first eight residues are more flexible than the last five because the latter are located at beta strand f. (For interpretation of the references to colour in this figure legend, the reader is referred to the web version of this article.)

dues close to the disulfide area (residues 1 to 5 and 16 to 17) are less ordered than the middle region comprising the TPEGAEA sequence (residues 6–11). This different behavior in terms of flexibility is corroborated by the D_2O exchange rate observed when the

lyophilized peptide is directly dissolved in D_2O. Whereas the amides of the 1–5 and 16–17 regions are immediately exchanged, those corresponding to the central part are partially protected from exchange, thereby indicating that these amide groups participate

P. Martin-Malpartida, S. Arrastia-Casado, J. Farrera-Sinfreu et al.

Computational and Structural Biotechnology Journal 20 (2022) 2082–2090

to some extent in hydrogen bonds. The backbone orientation of this central portion adopts a β-hairpin conformation, similar to that of the native protein (Fig. 3B). The similarity is extended to the preferred side-chain orientations of the Thr6, Glu8 and Glu11, which are essential for the alveolar fluid clearance capacity of the lectin-like domain of TNF, and whose similar orientation probably accounts for the capacity of the peptide to mimic the protein function. The conformational ensemble displayed by the peptide in solution (Fig. 3C) recapitulates the significant differences in Phi and Psi values observed when comparing the TIP region in seven X-ray structures of the hTNF cytokine (Fig. 3D). These differences suggest that the crystal structures of hTNF have trapped some conformational flexibility present in the context of the native protein, which is essential for recognizing various targets.

Given that 35% of solnatide residues are polar, we also studied the charge distribution of the peptide in solution. As shown in Fig. 4A, there are two observable electrostatic charged poles: a negatively charged site, centered at the β-hairpin defined by Glu8 and Glu11, and a positively charged one, defined by Arg4 and Lys13 side-chains. The negatively charged patch is also present in the TIP region of the hTNF cytokine (Fig. 4B). We also observed that the peptide shows a small semi-hydrophobic core (Fig. 4A), with the aromatic ring of Trp15 populating several orientations, defined by the interactions with neighbouring residues and by the turn introduced by the cyclic structure. In the native TNF structure, this turn is not present and these residues adopt an alternating orientation since they are located in the βf strand (Fig. 1A). The presence of the peptide core does not compromise its solubility and might even strengthen the interactions with the natural binders in a cellular context. These interactions could involve the stacking of sugar molecules against the planar face of Trp and Tyr, as observed in other proteins [49], interactions that can be further stabilized by hydrogen bonding partners such as the Gln3 and Glu5 sidechains located in close proximity.

3.4. Modeling solnatide-ENaCα interactions

The heterotrimeric ENaC channel has a large, well-structured extracellular region [26], a narrow transmembrane domain composed of two transmembrane helices per subunit, named TM1 and TM2, and a flexible C-terminal cytoplasmic domain [18]. In vitro, the solnatide binding site in ENaCα has been mapped to involve the region after transmembrane motif 2 (TM2), in the cytoplasmic face of the channel and in the C-terminal domain, in the proximity of residues 567 and 568 [11,23] and before the PPxY

motif (Fig. 5A). This motif interacts with the WW domains [50] of the ubiquitin ligase Nedd4L, which labels ENaCα for degradation [51].

The fragment used to determine the cryoEM structure of the ENaCα subunit ends after the TM2 helix, but the folded part ends early, the ENaCα region proposed to bind the solnatide peptide being absent. Although the structural properties of the C-terminal region await adequate experimental support, secondary structural prediction using JPred4 [52] and also AlphaFold_v2 [53], reveal that the region after the TM2 helix that was described as solnatide binding site (∼30 residues) has a high propensity to adopt a helical secondary structure. To represent these structural features, we overlapped the cryoEM structure of ENaC heterotrimer to the ENaCα model generated by AlphaFold_v2, including the predicted SB helix (highlighted in dark brown, in Fig. 5A). Moreover, this helical segment (SB helix, residues 563–595), has an amphipathic character as predicted by HELIQUEST [54], which is reflected by the segregation of hydrophobic and hydrophilic/charged residues occupying opposite faces of the helix, as shown in Fig. 5A,B.

In addition, in the helical conformation, charged residues are also separated as a small dipole, with negatively and positively charged residues clustered at the N and C ends of the helix, respectively. Since solnatide also has positively and negatively charged patches and a small hydrophobic core, it is tempting to hypothesize a binding process driven by complementary electrostatic and hydrophobic interactions between both molecules. To explore these potential interactions, we used RosettaDock r280, the SB helix predicted by AlphaFold_v2 and the minimum-energy NMR conformer of solnatide. As explained in the methods, we did not select any preferred starting orientation for the molecular docking. However, since the protocol was run without using a lipidic membrane, all simulations that oriented the peptide at the hydrophobic side of the helix were discarded. The complex with the lowest energy indicates that solnatide can interact with both positively and negatively charged patches of the SB helix oriented towards the cytoplasm (Fig. 5b), suggesting a possible binding mechanism of ENaCα recognition. Of note, although the C-terminal domain of the ENaCα subunit is less conserved than the extracellular domain and the transmembrane helices, the negatively charged residues surrounding the TM2 helix and the positively charged region in the SB helix are highly conserved in vertebrates [18].
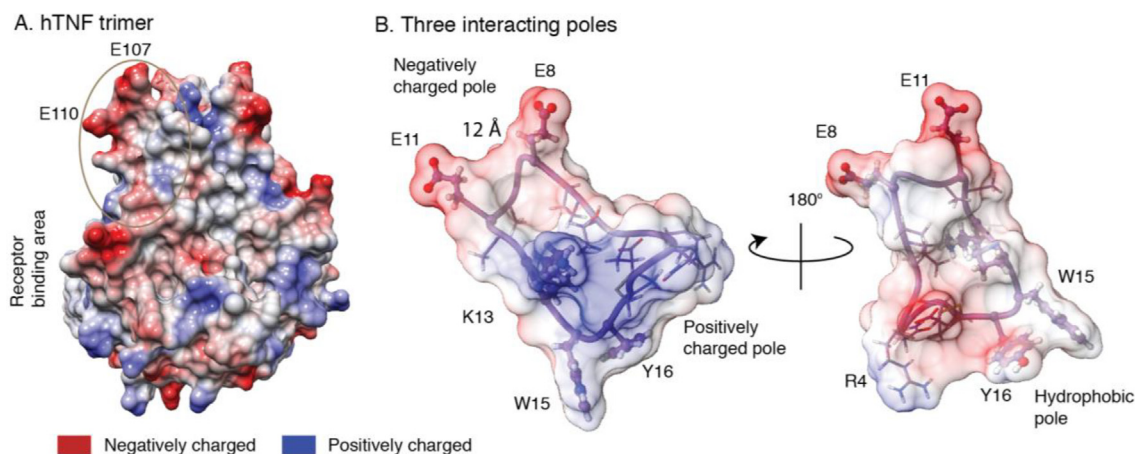
Fig. 4. Electrostatic surfaces of hTNF and solnatide. A. Charge distribution for the hTNF heterotrimer. The region similar to solnatide is circled. B. Charge distribution of the conformer shown in Fig. 3B. Two views related by a 180 rotation are represented. The negatively and positively charged areas and the hydrophobic pole are labeled.
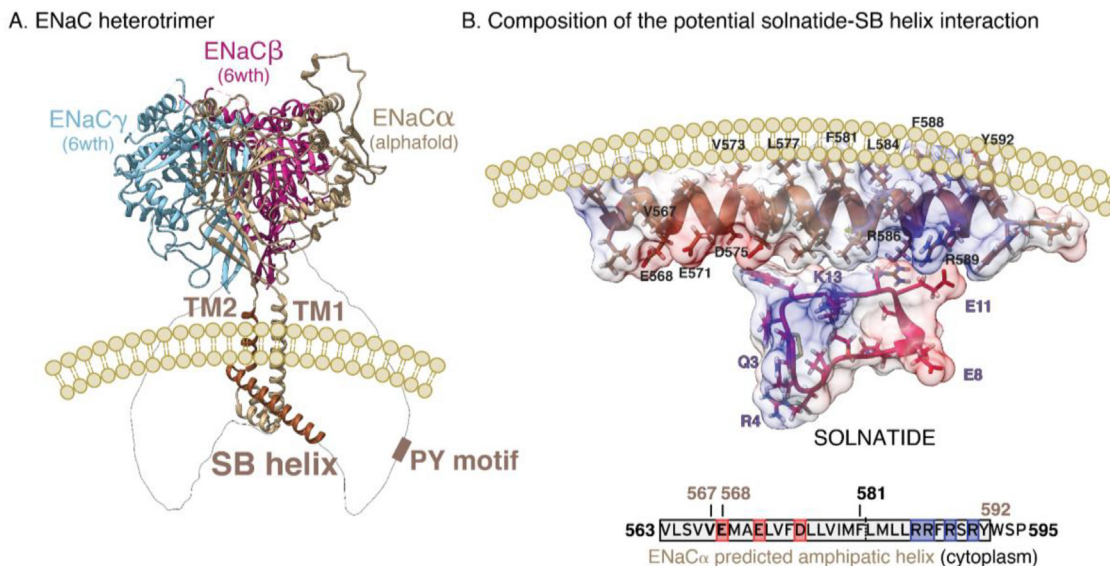
Fig. 5. Proposed model of solnatide interaction with the C-terminal helix of the ENaCα. A. ENaC heterotrimer as observed in the cryoEM structure. The cytoplasmic helical segment after the TM2 domain is shown in dark brown. This region is not present in the cryoEM structure but has been predicted by AlphaFold [53]. B. Expanded view of the cytoplasmic helical segment predicted by AlphaFold. A possible scenario for the recognition of the C-terminal helix and solnatide, obtained using RosettaDock. The presence of two charged patches at the SB helix and solnatide suggests that these areas could contribute to target recognition through electrostatic interactions via electrostatic complementarity. Binding to the positively charged patches (residues Arg585-Arg589) should be also satisfied by TNF native protein.

4. Discussion

Peptide therapeutics represent a well-defined area in the pharmaceutical industry. There are currently more than 80 approved peptide drugs on the market in the US, Europe and Japan, 150 in clinical development, and twice as many in preclinical studies https://www.fda.gov, [55,56]. Examples include numerous venom-derived peptides, with direct therapeutic applications for chronic pain, diabetes, stroke, and autoimmune diseases and cancer [57]. Other examples include insulin [58] and modifications of native hormones to optimize analogs with improved stability and specificity, like somatostatin, octreotide, leuprolide, and icatibant, to name a few. Some of these improvements have been made possible by exploring the conformational space sampled by the native peptides in solution [30,32,59,60].

Solnatide, the 17-residue synthetic cyclic peptide, is based on the native human TNF sequence and has lectin-like activity, i.e., it binds to specific carbohydrate groups on protein target molecules. The use of TNF to treat cancer has been hampered by its high hepatotoxicity and systemic toxicity [61] but the lectin-like domain of TNF, which is spatially distinct from the receptor binding sites, might have applications in reducing the formation of pulmonary edema associated with cancer treatment [6]. The function of the lectin-like domain of TNF has been preserved in the synthetic cyclic peptide solnatide, which contains the sequence of residues corresponding to the lectin-like domain of human TNF, constrained by a disulfide bond between the N- and C- termini. The ability of both solnatide and TNF to reabsorb edema and the trypanolytic effects of the lectin-like domain are lost when residues Thr6/105, Glu8/107 and Glu11/110 (solnatide and TNF numbering respectively), are each replaced by alanine [3,10,12,13]. In contrast to the considerable number of structural studies available for TNF proteins in the literature [2,44], the folding properties of solnatide have not been explored to date.

This lack of conformational information has not only limited the capacity to describe the mechanism of action of solnatide but also compromised efforts to improve its stability and/or membrane and ENaC association properties through chemical modification. Here

we found that solnatide has retained 3D features of the lectin-like domain of TNF required for function. In fact, the analysis of the conformational ensembles displayed by solnatide shows how the peptide recapitulates the main structural features previously identified as relevant for the ENaC-activating effect of the lectin-like domain of TNF [12,13], namely the critical role of the triad of residues in solnatide/hTNF: Thr6/105, Glu8/107 and Glu11/110, the hydrophobic region comprising three consecutive residues Pro14/113, Trp15/115 and Tyr16/115, and the presence of a charged dipole, all of which are observed in the peptide. The middle region of solnatide, represented by the sequence TPEGAEA, is ordered, shows H-bonding capacity, and adopts a backbone conformation similar to that of the native protein.

Two residues (Val567 and Glu568) at the C-terminal region of human ENaCα play an important role in solnatide binding *in vitro*. This conclusion is based on the observation that mutation of these residues to alanine significantly reduces the stimulatory effect of the peptide on the interaction between ENaC and the myristoylated alanine-rich C kinase substrate MARCKS. These mutations also affect ENaCα activation in H441 cells by hTNF [23].

Based on the conformational studies and in the analysis of charge distribution of the peptide surface reported here, we propose a model to describe how solnatide may interact with the cytoplasmic C-terminal domain of the ENaCα subunit via electrostatic complementarity. Remarkably, both the amphipathic helix and solnatide have positively and negatively charged patches. Assuming that the hydrophilic face of the SB helix interacts with the membrane and that the polar surface is oriented to the cytoplasm, this polar face would be accessible to interact with solnatide through complementary electrostatic interactions, involving binding to the negatively and positively charged patches (residues Glu568, Glu571 and Asp575 and Arg585-Arg589). Our model generated with RosettaDock supports the implication of a slightly larger area of the SB helix than previously thought, including a short patch of positively charged residues located at the C-terminal part of the SB helix. This hypothesis still needs further experimental validation, but if confirmed, it may help the future development of new generations of solnatide analogues to enhance the capabilities of this

P. Martin-Malpartida, S. Arrastia-Casado, J. Farrera-Sinfreu et al.

Computational and Structural Biotechnology Journal 20 (2022) 2082–2090

scaffold and/or to acquire new properties including the formation of dimers or trimers to mimic the native trimeric TNF structure. In addition, a technical application of the peptide-SB interaction may be used as a tool for structural determination of the cytoplasmic region of ENaC, which has been invisible in the cryo-EM structures until now. In this context, the addition of the peptide during the protein reconstitution for structural studies might help restrict the orientation of the otherwise dynamic SB helix, thereby facilitating its observation in these models.

We are confident that the conformational properties of solnatide gained through the present study paves the way for further studies addressing the differences observed between the peptide and its parent molecule TNF with respect to ENaC activation characteristics [24] and might allow a glimpse into the evolutionary mechanisms that led to a moonlighting protein like TNF.

5. Coordinates and NMR assignments

PDB ID 7QLF, BMRB ID 34697.

CRediT authorship contribution statement

Pau Martin-Malpartida: Methodology, Formal analysis, Investigation, Visualization, Writing – original draft. **Silvia Arrastia-Casado:** Methodology, Resources, Writing – review & editing. **Josep Farrera-Sinfreu:** Methodology, Resources, Writing – review & editing. **Rudolf Lucas:** Writing – review & editing. **Hendrik Fischer:** Project administration, Writing – review & editing. **Bernhard Fischer:** Conceptualization, Resources, Project administration, Funding acquisition, Writing – review & editing. **Douglas C. Eaton:** Writing – review & editing. **Susan Tzotzos:** Writing – original draft, Visualization, Writing – review & editing. **Maria J. Macias:** Conceptualization, Methodology, Formal analysis, Investigation, Supervision, Visualization, Writing – original draft, Writing – review & editing.

Conflict of interest

RL is inventor on several patents related to the use of solnatide in edema reabsorption, ST, BF and HF are employees of Apeptico GmbH.

The remaining authors declare no competing interests. Neither the EC nor the FFG had any role in the design of the research, collection, analysis, and interpretation of data or in writing the manuscript.

Acknowledgements

Appendix A. Supplementary data

References

[1] Braun C, Hamacher J, Morel DR, Wendel A, Lucas R. Dichotomal role of TNF in experimental pulmonary edema reabsorption. J Immunol 2005;175:3402–8.
[2] Eck MJ, Sprang SR. The structure of tumor necrosis factor-alpha at 2.6 A resolution. Implications for receptor binding. J Biol Chem 1989;264:17595–605.
[3] Lucas R, Magez S, De Leys R, Fransen L, Scheerlinck JP, Rampelberg M, et al. Mapping the lectin-like activity of tumor necrosis factor. Science 1994;263:814–7.
[4] Yang G, Hamacher J, Gorshkov B, White R, Sridhar S, Verin A, et al. The dual role of TNF in pulmonary edema. J Cardiovasc Dis Res 2010;1:29–36.
[5] Lucas R, Hadizamani Y, Enkhbaatar P, Csanyi G, Caldwell RW, Hundsberger H, et al. Dichotomous role of tumor necrosis factor in pulmonary barrier function and alveolar fluid clearance. Front Physiol 2022;12:30.
[6] Hundsberger H, Verin A, Wiesner C, Pfluger M, Dulebo A, Schutt W, Lasters I, Mannel DN, Wendel A, Lucas R. TNF: a moonlighting protein at the interface between cancer and infection. Front Biosci 2008;13:5374–86.
[7] Aggarwal BB, Gupta SC, Kim JH. Historical perspectives on tumor necrosis factor and its superfamily: 25 years later, a golden journey. Blood 2012;119:651–65.
[8] Dostert C, Grusdat M, Letellier E, Brenner D. The TNF family of ligands and receptors: communication modules in the immune system and beyond. Physiol Rev 2019;99:115–60.
[9] Hribar M, Bloc A, van der Goot FG, Fransen L, De Baetselier P, Grau GE, et al. The lectin-like domain of tumor necrosis factor-alpha increases membrane conductance in microvascular endothelial cells and peritoneal macrophages. Eur J Immunol 1999;29:3105–11.
[10] Fukuda N, Jayr C, Lazrak A, Wang Y, Lucas R, Matalon S, et al. Mechanisms of TNF-alpha stimulation of amiloride-sensitive sodium transport across alveolar epithelium. Am J Physiol Lung Cell Mol Physiol 2001;280:L1258–1265.
[11] Czikora I, Alli A, Bao HF, Kaftan D, Sridhar S, Apell HJ, et al. A novel tumor necrosis factor-mediated mechanism of direct epithelial sodium channel activation. Am J Respir Crit Care Med 2014;190:522–32.
[12] Hazemi P, Tzotzos SJ, Fischer B, Andavan GS, Fischer H, Pietschmann H, et al. Essential structural features of TNF-alpha lectin-like domain derived peptides for activation of amiloride-sensitive sodium current in A549 cells. J Med Chem 2010;53:8021–9.
[13] Elia N, Tapponnier M, Matthay MA, Hamacher J, Pache JC, Brundler MA, et al. Functional identification of the alveolar edema reabsorption activity of murine tumor necrosis factor-alpha. Am J Respir Crit Care Med 2003;168:1043–50.
[14] Vadasz I, Schermuly RT, Ghofrani HA, Rummel S, Wehner S, Muhldorfer I, et al. The lectin-like domain of tumor necrosis factor-alpha improves alveolar fluid balance in injured isolated rabbit lungs. Crit Care Med 2008;36:1543–50.
[15] Krenn K, Lucas R, Croize A, Boehme S, Klein KU, Hermann R, et al. Inhaled AP301 for treatment of pulmonary edema in mechanically ventilated patients with acute respiratory distress syndrome: a phase IIa randomized placebo-controlled trial. Crit Care 2017;21:194.
[16] Aigner C, Slama A, Barta M, Mitterbauer A, Lang G, Taghavi S, et al. Treatment of primary graft dysfunction after lung transplantation with orally inhaled AP301: A prospective, randomized pilot study. J Heart Lung Transplant 2017.
[17] Eaton DC, Helms MN, Koval M, Bao HF, Jain L. The contribution of epithelial sodium channels to alveolar function in health and disease. Annu Rev Physiol 2009;71:403–23.
[18] Hanukoglu I, Hanukoglu A. Epithelial sodium channel (ENaC) family: Phylogeny, structure-function, tissue distribution, and associated inherited diseases. Gene 2016;579:95–132.
[19] Shabbir W, Scherbaum-Hazemi P, Tzotzos S, Fischer B, Fischer H, Pietschmann H, et al. Mechanism of action of novel lung edema therapeutic AP301 by activation of the epithelial sodium channel. Mol Pharmacol 2013;84:899–910.
[20] Tzotzos S, Fischer B, Fischer H, Pietschmann H, Lucas R, Dupre G, et al. AP301, a synthetic peptide mimicking the lectin-like domain of TNF, enhances amiloride-sensitive Na(+) current in primary dog, pig and rat alveolar type II cells. Pulm Pharmacol Ther 2013;26:356–63.
[21] Hummler E, Barker P, Gatzy J, Beermann F, Verdumo C, Schmidt A, et al. Early death due to defective neonatal lung liquid clearance in alpha-ENaC-deficient mice. Nat Genet 1996;12:325–8.
[22] Kleyman TR, Eaton DC. Regulating ENaC's gate. Am J Physiol Cell Physiol 2020;318:C150–62.
[23] Lucas R, Yue Q, Alli A, Duke BJ, Al-Khalili O, Thai TL, et al. The lectin-like domain of TNF increases ENaC open probability through a novel site at the interface between the second transmembrane and C-terminal domains of the alpha-subunit. J Biol Chem 2016;291:23440–51.
[24] Willam A, Aufy M, Tzotzos S, El-Malazi D, Poser F, Wagner A, et al. TNF lectin-like domain restores epithelial sodium channel function in frameshift mutants associated with pseudohypoaldosteronism type 1B. Front Immunol 2017;8:601.
[25] Berthiaume Y, Matthay MA. Alveolar edema fluid clearance and acute lung injury. Respir Physiol Neurobiol 2007;159:350–9.

P. Martin-Malpartida, S. Arrastia-Casado, J. Farrera-Sinfreu et al.

Computational and Structural Biotechnology Journal 20 (2022) 2082–2090

[26] Noreng S, Bharadwaj A, Posert R, Yoshioka C, Baconguis I. Structure of the human epithelial sodium channel by cryo-electron microscopy. Elife 2018;7.

[27] Noreng S, Posert R, Bharadwaj A, Houser A, Baconguis I. Molecular principles of assembly, activation, and inhibition in epithelial sodium channel. Elife 2020;9.

[28] Shabbir W, Tzotzos S, Bedak M, Aufy M, Willam A, Kraihammer M, et al. Glycosylation-dependent activation of epithelial sodium channel by solnatide. Biochem Pharmacol 2015;98:740–53.

[29] Marquardt A, Bernevic B, Przybylski M. Identification, affinity characterisation and biological interactions of lectin-like peptide-carbohydrate complexes derived from human TNF-alpha using high-resolution mass spectrometry. J Pept Sci 2007;13:803–10.

[30] Martin-Gago P, Gomez-Caminals M, Ramon R, Verdaguer X, Martin-Malpartida P, Aragon E, et al. Fine-tuning the pi-pi aromatic interactions in peptides: somatostatin analogues containing mesityl alanine. Angew Chem Int Ed Engl 2012;51:1820–5.

[31] Martin-Gago P, Ramon R, Aragon E, Fernandez-Carneado J, Martin-Malpartida P, Verdaguer X, et al. A tetradecapeptide somatostatin dicarba-analog: Synthesis, structural impact and biological activity. Bioorg Med Chem Lett 2014;24:103–7.

[32] Rol A, Todorovski T, Martin-Malpartida P, Escola A, Gonzalez-Rey E, Aragon E, et al. Structure-based design of a Cortistatin analogue with immunomodulatory activity in models of inflammatory bowel disease. Nat Commun 2021;12:1869.

[33] Bax A. MLEV-17-based two-dimensional homonuclear magnetization transfer spectroscopy. J Magn Reson 1985;65:355–60.

[34] Macura S, Ernst RR. Elucidation of cross relaxation in liquids by two-dimensional NMR spectroscopy. Mol Phys 1980;41:95–117.

[35] Macias MJ, Musacchio A, Ponstingl H, Nilges M, Saraste M, Oschkinat H. Structure of the pleckstrin homology domain from beta-spectrin. Nature 1994;369:675–7.

[36] Wüthrich K. NMR of proteins and nucleic acids. New York: Wiley; 1986. p. 1.

[37] Keller RLJ. The computer aided resonance assignment tutorial CARA. Cantina Verlag; 2004.

[38] Brunger AT. Version 1.2 of the Crystallography and NMR system. Nat Protoc 2007;2:2728–33.

[39] Brunger AT, Adams PD, Clore GM, DeLano WL, Gros P, Grosse-Kunstleve RW, et al. Crystallography & NMR system: A new software suite for macromolecular structure determination. Acta Crystallogr D Biol Crystallogr 1998;54:905–21.

[40] Ramirez-Espain X, Ruiz L, Martin-Malpartida P, Oschkinat H, Macias MJ. Structural characterization of a new binding motif and a novel binding mode in group 2 WW domains. J Mol Biol 2007;373:1255–68.

[41] Mao B, Tejero R, Baker D, Montelione GT. Protein NMR structures refined with Rosetta have higher accuracy relative to corresponding X-ray crystal structures. J Am Chem Soc 2014;136:1893–906.

[42] Pettersen EF, Goddard TD, Huang CC, Couch GS, Greenblatt DM, Meng EC, et al. UCSF Chimera–a visualization system for exploratory research and analysis. J Comput Chem 2004;25:1605–12.

[43] Marze NA, Roy Burman SS, Sheffler W, Gray JJ. Efficient flexible backbone protein-protein docking for challenging targets. Bioinformatics 2018;34:3461–9.

[44] Jones EY, Stuart DI, Walker NP. Structure of tumour necrosis factor. Nature 1989;338:225–8.

[45] Martin OA, Villegas ME, Vila JA, Scheraga HA. Analysis of 13Calpha and 13Cbeta chemical shifts of cysteine and cystine residues in proteins: a quantum chemical approach. J Biomol NMR 2010;46:217–25.

[46] Sala D, Huang YJ, Cole CA, Snyder DA, Liu G, Ishida Y, et al. Protein structure prediction assisted with sparse NMR data in CASP13. Proteins 2019;87:1315–32.

[47] Linge JP, Williams MA, Spronk CA, Bonvin AM, Nilges M. Refinement of protein structures in explicit solvent. Proteins 2003;50:496–506.

[48] Laskowski RA, Rullmannn JA, MacArthur MW, Kaptein R, Thornton JM. AQUA and PROCHECK-NMR: programs for checking the quality of protein structures solved by NMR. J Biomol NMR 1996;8:477–86.

[49] Houser J, Kozmon S, Mishra D, Mishra SK, Romano PR, Wimmerova M, et al. Influence of Trp flipping on carbohydrate binding in lectins. An example on Aleuria aurantia lectin AAL. PLoS One 2017;12:e0189375.

[50] Macias MJ, Wiesner S, Sudol M. WW and SH3 domains, two different scaffolds to recognize proline-rich ligands. FEBS Lett 2002;513:30–7.

[51] Rotin D, Staub O. Nedd4-2 and the regulation of epithelial sodium transport. Front Physiol 2012;3:212.

[52] Drozdetskiy A, Cole C, Procter J, Barton GJ. JPred4: a protein secondary structure prediction server. Nucleic Acids Res 2015;43:W389–394.

[53] Jumper J, Evans R, Pritzel A, Green T, Figurnov M, Ronneberger O, et al. Highly accurate protein structure prediction with AlphaFold. Nature 2021;596:583–9.

[54] Gautier R, Douguet D, Antonny B, Drin G. HELIQUEST: a web server to screen sequences with specific alpha-helical properties. Bioinformatics 2008;24:2101–2.

[55] Lau JL, Dunn MK. Therapeutic peptides: Historical perspectives, current development trends, and future directions. Bioorg Med Chem 2018;26:2700–7.

[56] Muttenthaler M, King GF, Adams DJ, Alewood PF. Trends in peptide drug discovery. Nat Rev Drug Discov 2021;20:309–25.

[57] King GF. Venoms as a platform for human drugs: translating toxins into therapeutics. Expert Opin Biol Ther 2011;11:1469–84.

[58] Sanger F. Sequences, sequences, and sequences. Annu Rev Biochem 1988;57:1–28.

[59] Martin-Gago P, Aragon E, Gomez-Caminals M, Fernandez-Carneado J, Ramon R, Martin-Malpartida P, et al. Insights into structure-activity relationships of somatostatin analogs containing mesitylalanine. Molecules 2013;18:14564–84.

[60] Martin-Gago P, Rol A, Todorovski T, Aragon E, Martin-Malpartida P, Verdaguer X, et al. Peptide aromatic interactions modulated by fluorinated residues: Synthesis, structure and biological activity of Somatostatin analogs containing 3-(3',5'difluorophenyl)-alanine. Sci Rep 2016;6:27285.

[61] Spriggs DR, Sherman ML, Michie H, Arthur KA, Imamura K, Wilmore D, et al. Recombinant human tumor necrosis factor administered as a 24-hour intravenous infusion. A phase I and pharmacologic study. J Natl Cancer Inst 1988;80:1039–44.